

# Strong Field Limit Lensing Effects in the Minimal Geometric Deformation and Casadio-Fabbri-Mazzacurati Solutions

R. T. Cavalcanti\* and A. Goncalves da Silva†

*Centro de Ciências Naturais e Humanas,  
Universidade Federal do ABC,  
09210-580, Santo André - SP, Brazil*

Roldão da Rocha‡

*Centro de Matemática, Computação e Cognição,  
Universidade Federal do ABC,  
09210-580, Santo André - SP, Brazil.*

(Dated: June 2, 2022)

In this paper we apply the strong field limit approach to investigate the gravitational lensing beyond general relativity. It is accomplished by considering the lensing effects related to black hole solutions emerging out of the domain of Einstein gravity, namely, the ones acquired from the method of geometric deformation and the Casadio-Fabbri-Mazzacurati brane-world black holes. The lensing observables, for those brane-world black hole metrics, are compared with the ones for the Schwarzschild case. We prove that brane-world black holes could have significantly different observational signatures, compared to the Schwarzschild black hole, with terms containing the post-Newtonian parameter, for the case of the Casadio-Fabbri-Mazzacurati, and the variable brane-world tension, for the method of geometric deformation.

PACS numbers: 04.50.+h, 04.70.Bw, 95.30.Sf, 98.62.Sb

Keywords: Minimal geometric deformation; black holes; gravitational lensing; brane-worlds, CFM metrics

## I. INTRODUCTION

Black hole solutions of the Einstein equations in general relativity (GR) are useful tools for investigating the spacetime structure, the collapse of compact stellar distributions, and quantum effects in theories of gravity. In particular, extended models of GR [1] lead to important consequences, not only to black hole physics [2], but also to particle physics, cosmology, and to the astrophysics of supermassive objects [3]. Hence, exploring the gravitational phenomena, in which these consequences come to light, provides a way to pave extended models, as well as to test the limits of GR. The gravitational lensing represents one of those phenomena. The deflection of light by a gravitational potential was first observed in 1919 by Dyson, Eddington and Davidson [4], whose modern refinements has become one of the experimental grounds of GR. Thereafter, the deflection of light was found to imply lens effects, that could magnify or create multiple images of astrophysical objects [5]. This was a landmark for a contemporary field of research, known as gravitational lensing (GL). The works of Liebes [6] and Refsdal [7] developed the theory of gravitational lensing in the so-called weak field limit, where the lens equations and the expression for the deflection angle are quite simplified, hence allowing one to solve them exactly. The predic-

tions of the theory, in this regime, have been thoroughly supported by experiments. It is worth to mention, for example, the observation of twin quasars separated by arc-seconds (as), however at same redshifts and magnitudes [8], images of distorted galaxies inside another galaxy [9], among others [10]. With all this success in the weak field limit, the question about what happens in the strong field regime was driven by the possibility of existence of galactic supermassive black holes at the centre of our galaxy. The subject was brought back by Virbhadra and Ellis [11], that theoretically investigated the strong field region of a Schwarzschild type lens. They found that, in the strong field regime, the theory predicts a large number of images of an observed object – theoretically, an infinite sequence of images, with an adherent point. The result contrasts with a pair of images, or an Einstein ring, predicted in the weak field limit regime. Following the work of Virbhadra and Ellis, Bozza [12, 13] has found an interesting simplification for the lens equation in such regime, finding the expression for observables quantities in the so-called strong field limit (SFL) regime. Bozza proved that, when the angle between the source and the lens tends to zero, the deflection angle diverges logarithmically. Furthermore, it can be integrated up to first order, wherefrom the GL observables can be derived.

In a series of papers, Keeton and Petters studied a general framework for the weak field limit, comprising the case of a static and spherically symmetric solution [14], the post-Newtonian metrics [15] and brane-world gravity [16]. Whisker has considered gravitational lensing at strong field limit [17], as a way to seek for signatures of a solutions of five-dimensional (5D) brane-world gravity.

---

\*Electronic address: rogerio.cavalcanti@ufabc.edu.br

†Electronic address: allan.goncalves@ufabc.edu.br

‡Electronic address: roldao.rocha@ufabc.edu.br

For some 5D brane-world solutions, the difference in the observables were found to be very small from the four-dimensional (4D) Schwarzschild case. Thereafter, Bozza revised the theoretical and observational aspects of gravitational lensing produced by black holes [18].

In this paper, we apply the SFL to obtain the GL observables for two remarkable black holes solutions beyond GR, namely the Casadio-Fabbri-Mazzacurati and the minimal geometric deformation. Solutions of the Einstein field equations in 5D gravity, in brane-world models, are not, in general, univocally governed just by the matter stress-tensor. Indeed, gravity can propagate into the bulk, hence generating a Weyl term on the brane, accordingly [1]. The Casadio-Fabbri-Mazzacurati (CFM) metrics generalise the Schwarzschild solution and have a parametrised post-Newtonian (PPN) form, with parameter  $\delta \approx 1$ . The PPN measures, in particular, the difference between the inertial and the gravitational masses and, furthermore, affects perihelia shifts and accounts Nordtvedt effect, as moreover constrained by the Lunar Laser Ranging Experiment (LLRE) [19–21]. The PPN  $\delta$  allows comparing experimental data in the weak-field limit, which is adequately accurate, in order to include solar system tests [21]. In fact, the parameter  $\delta$  is the usual Eddington-Robertson-Schiff parameter used to describe the classical tests of GR. The minimal geometric deformation (MGD), on the other hand, was introduced in the context of investigating the outer spacetime around (spherically symmetric) self-gravitating systems. It includes stars or similar compact astrophysical objects [22] likewise, in Randall-Sundrum-like brane-world setups. To solve the brane effective Einstein field equations is an intricate endeavour, whose analytical solutions are scarce in the literature [1]. The MGD naturally encompasses the (variable) brane tension, and has been employed to derive exact, physically feasible, solutions for spherically symmetric, for non-uniform, and inner stellar distributions, to generate other physical inner stellar solutions, and their microscopic counterparts, accordingly. MGD can be thought of being induced by non-local outer Weyl stresses that are evinced from bulk gravitons. In addition, the deformation of the time component of the metric has been recently accomplished, thus characterising the so-called extended MGD procedure [23]. The MGD further encompasses tidally charged metrics of extremal black hole with degenerate horizons, outer solutions for self-gravitating systems induced by 5D Weyl fluids – which can represent a Weyl atmosphere, accordingly [22–24]. Our aim in this paper is to derive and analyse the gravitational lensing effects regarding the CFM and MGD solutions.

The paper is organised as follows. In Sect. II we introduce the fundamental equations and the underlying physical framework of the gravitational lensing, mainly focusing on the SFL regime. In Sect. III, we briefly revisit the MGD as well as the CFM solutions, in order to fix the notation and to define the main setup that shall be further analysed. Sect. IV is devoted to the observable

quantities in the SFL regime, containing our results and their analysis, for the solutions discussed in the Sect. III. To conclude, in Sect. V we summarise the results, point out our concluding remarks and perspectives, and discuss the possibility of detection/observation of signatures of the MGD and CFM solutions.

## II. GRAVITATIONAL LENSING AND THE STRONG FIELD LIMIT (SFL)

The correct prediction of the light deflection angle by the Sun is one of the greatest and earliest achievements of GR. Gravitational lensing regards the deflection of light through a gravitational field, being related with, for instance, the Hubble constant and cosmological constant, among others, arising as an important tool to probe the physical properties of astrophysical objects. The general setup of a gravitational lens is depicted in Fig. 1. The light of a source  $S$  is deflected when it passes by a lens  $L$ . The image of  $S$  appears to the observer  $O$ , in a position characterised by the angle  $\theta$ , instead of the angle  $\beta$ , and the deflection angle  $\alpha$  [25]. The lens equation, relating these angles, reads

$$\tan \beta = \tan \theta - \frac{D_{Ls}}{D_{os}} [\tan \theta - \tan (\theta - \alpha)]. \quad (1)$$

Hence, an object position  $\beta$  provides the angle  $\alpha$ , in order to solve Eq. (1) for the image position  $\theta$ . Basic assumptions are that the lens effect is induced by local matter inhomogeneities and the source and the observer are in an asymptotic flat spacetime. The integration of the null geodesic [26], associated with the angular deflection as a function of radial distance  $r$ , in the vicinity of a metric

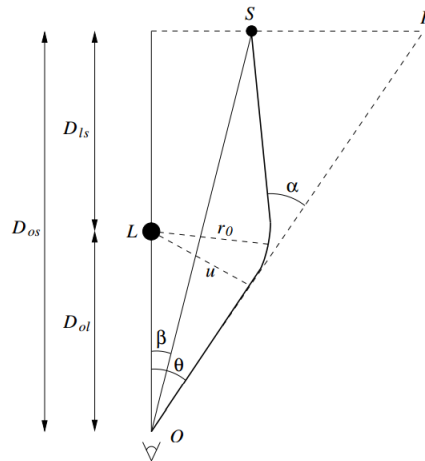


FIG. 1: Gravitational lensing setup (in Ref. [17].) The distance  $r_0$  is the closest approximation of the light rays to the lens, and  $u$  denotes the impact parameter.

$$ds^2 = A(r)dt^2 - B(r)dr^2 - r^2d\Omega^2, \quad (2)$$

yields

$$\alpha(r) = \int_r^\infty \frac{B(r)^{1/2}}{r} \left[ \left( \frac{r}{r_0} \right)^2 \left( \frac{A(r_0)}{A(r)} \right) - 1 \right]^{1/2} dr. \quad (3)$$

In the weak field regime, corresponding to the light passing far way from the compact object event horizon, the angles in Eq. (8) can be expanded to the first order. In the particular scenario of the Schwarzschild solution, the deflection reads  $\alpha(r_0) = \frac{4GM}{c^2 r_0}$ , and two antipode images are observed. The separation between these two images is the well-known Einstein radius  $\theta_E = \frac{2}{c} \sqrt{\frac{GM D_{ls}}{D_{os} D_{ol}}}$ . When the lens and the source are aligned,  $\beta = 0$ , a ring of radius  $\theta_E$ , known as the Einstein ring, is formed around the lens.

Here we are interested in the full non-linear regime of GR, that translates in considering the light trajectory near the event horizon. In this setup, the deflection angle increases and, for some impact parameter, becomes larger than  $2\pi$ , meaning a photon looping around the black hole, before travelling towards the observer. The images originated from those photons are known as relativistic images [11]. If one continues to decrease the impact parameter, the number of loops shall increase until  $\alpha$  diverges, and the photon crosses the event horizon. Therefore, instead of a image at each side of lens that appear in the weak field regime, the observer sees infinite sequence of images on each side of the lens [12]. The so-called *photon sphere*  $r_m$ , defining unstable orbits around the black hole [27], is the largest solution of the equation  $(\ln A(r))' = 1/r$ , and the correspondent impact parameter reads  $u_m = r_m/A(r_m)$ . As the closest approximation  $r_0$  goes to the photon sphere, the deflection angle diverges logarithmically [13]. Doing the appropriate expansion around  $r_m$ , the expression for the deflection angle, in the so called strong field limit (SFL), reads [13]

$$\alpha(\theta) = -\bar{a} \ln \left( \frac{\theta D_{ol}}{u_m} - 1 \right) + \bar{b} + \mathcal{O}(u - u_m), \quad (4)$$

where  $\mathcal{O}(u - u_m)$  represents higher order terms, and  $\bar{a}$ ,  $\bar{b}$  are the SFL coefficients that depend upon  $r$ ,  $A(r)$  and  $B(r)$ , calculated at the point  $r_m$ :

$$\bar{a} = \frac{R(0, r_m)}{2\sqrt{\mathfrak{b}}}, \quad (5)$$

$$\bar{b} = \bar{a} \ln \left( \frac{2\mathfrak{b}}{A(r_m)} \right) + b_R - \pi, \quad (6)$$

where

$$R(z, r_0) = \frac{2\sqrt{B(r)A(r)}}{rA'(r)} (1 - A(r_0)), \quad (7)$$

$$z = \frac{A(r) - A(r_0)}{1 - A(r_0)}, \quad (8)$$

$$b_R = \int_0^1 [R(z, r_m) f(z, r_m) - R(0, r_m) f_0(z, r_m)] dz, \quad (9)$$

$$\mathfrak{b} = \frac{(1 - A(r))^2}{2r^4 A'^3(r)} \left[ -2r^3 A''(r) A(r) + 2r(1 - 4r) A'(r) A(r) + 4r^3 A'(r)^2 \right] \Big|_{r=r_0}, \quad (10)$$

and

$$f(z, r_0) = \left( A(r_0) - [(1 - A(r_0))z - A(r_0)] \frac{r_0^2}{r^2} \right)^{-1/2} \quad (11)$$

$$f_0(z, r_0) = (\mathfrak{b}z^2 + \mathfrak{a}z)^{-1/2} \quad (12)$$

being  $\mathfrak{a}$  given by

$$\mathfrak{a} = \frac{1 - A(r)}{r^2 A'(r)} [2rA(r) - r^2 A'(r)] \Big|_{r=r_0}. \quad (13)$$

In the above expression, all the functions of  $r$  are evaluated at  $r$ , obtained by inverting Eq. (8) [13]. The parameters  $\bar{a}$  and  $\bar{b}$  play a prominent role in measuring the angular difference from the outmost image and the adherent point related to the sequence of subsequent images. We shall better discuss the underlying physical properties of those parameters in our analysis of Sect. IV. Eq. (4), together with considerations regarding the angles  $\theta$ ,  $\beta$ , and  $\alpha$ , allows us to derive the observable quantities for the gravitational lensing, which shall be accomplished in Sect. IV.

In the next section we shall present the MGD and CFM metrics paradigm and physical motivation to, subsequently, study their gravitational lensing effects. In addition, we are going to analyse the modifications of this approach to the listed black holes in the literature [12, 13, 28], and references therein.

### III. MGD AND CFM METRICS

In this section we briefly present the main physical features regarding the minimal geometric deformation procedure and the CFM solutions.

#### A. The MGD procedure

In brane-world scenarios, the brane self-gravity is encrypted in the brane tension  $\sigma$ . The brane tension was previously bounded in the DMPR and CFM solutions, by the classical tests of GR [29]. In the MGD procedure context, the bound  $\sigma \gtrsim 5.19 \times 10^6 \text{ MeV}^4$  was obtained

[30], providing a stronger bound, contrasted to the one provided by cosmological nucleosynthesis. The MGD underlying geometry encompasses high-energy corrections, since  $\sigma^{-1/2}$  plays the role of the 5D fundamental length scale<sup>1</sup>. The MGD is a deformation of the Schwarzschild solution, and devises observational effects that are originated by the PPN parameter  $\zeta \simeq (\sigma^{-1/2}/R)^2$ , describing a 4D geometry that surrounds a star of radius  $R$ , located on the brane. Moreover, the MGD is naturally led to the Schwarzschild metric, when  $\sigma^{-1} \rightarrow 0$ . In order to proceed, the Einstein effective brane equations read [31]

$$G_{\mu\nu} = -\Lambda g_{\mu\nu} - \hat{T}_{\mu\nu}. \quad (14)$$

The effective energy-momentum tensor  $\hat{T}_{\mu\nu} = T_{\mu\nu} + E_{\mu\nu} + \frac{6}{\sigma} S_{\mu\nu}$  splits into the brane matter energy-momentum tensor ( $T_{\mu\nu}$ ), the high-energy Kaluza-Klein induced tensor ( $S_{\mu\nu}$ ) and non-local corrections induced by the electric component of the Weyl tensor ( $E_{\mu\nu}$ ). In particular, if brane-world matter is described by a perfect fluid with 4-velocity  $u^\mu$ , and  $h_{\mu\nu} = g_{\mu\nu} - u_\mu u_\nu$  is the projection tensor on the fluid, hence  $E_{\mu\nu} = \frac{6}{\sigma} [Q_{(\mu} u_{\nu)} + P_{\mu\nu} + U (u_\mu u_\nu + \frac{1}{3} h_{\mu\nu})]$ , where  $Q_\mu$ ,  $U$ ,  $P_{\mu\nu}$  respectively denoting the energy flux, the bulk Weyl scalar, and the (anisotropic) stress. MGD metrics are exact solutions of Eq. (14) [22], yielding physical stellar inner solutions [24], having Schwarzschild outer solution that does not jet energy into the extra dimension [32]. 5D solutions were further obtained in various contexts [33, 34], providing models for the quasar luminosity variation and signatures from cosmic rays [3, 35].

The MGD, requiring that GR must be the low energy dominant regime  $\sigma^{-1} \rightarrow 0$ , derives a deformed radial component of the metric, by bulk effects, yielding [36]

$$B(r) = \nu(r) + f(r), \quad (15)$$

where (hereon we denote  $\frac{GM}{c^2} \mapsto M$ )

$$f(r) = e^{-I} \left( \int_0^r \frac{e^I}{\frac{A'^2}{2A^2} + \frac{2}{x}} \left[ H(p, \rho, A) + \frac{\rho^2 + 3\rho p}{\sigma} \right] dx + \zeta \right),$$

$$I(r) = \int_{r_0}^r \frac{\frac{A''A}{A'^2} - 1 + \frac{A'^2}{A^2} + \frac{2A'}{Ar} + \frac{1}{r^2}}{\frac{A'}{2A} + \frac{2}{r}} dr, \quad (16)$$

$$\nu(r) = 1 - \frac{2\dot{M}}{r}, \quad (17)$$

where  $\dot{M} = M$ , for  $r > R$ , or  $\dot{M} = m(r)$ , for  $r \leq R$ , where  $m(r) \equiv \frac{1}{2r} \int_0^r x^2 \rho dx$ , and  $M_0 = M|_{\sigma^{-1} \rightarrow 0}$ . The function  $H$  in Eq. (16),

$$H(p, \rho, A(r)) \equiv p - \left[ \frac{A'}{A} \left( \frac{B'}{2B} + \frac{1}{r} \right) + (\ln B - 1)r^{-2} + \ln B \left( \frac{A''A}{A'^2} - 1 + \frac{A'^2}{A^2} + \frac{2A'}{Ar} \right) \right] \quad (18)$$

encompasses anisotropic effects of bulk gravity, the pressure, and the density. In addition, in the region  $r < R$ , the constraint  $\zeta = \zeta(\sigma, r, M) = 0$  prevents singular solutions at  $r = 0$ , and perfect fluid solution of GR yields  $H(p, \rho, A(r)) = 0$ . To acquire the outer geometry by the MGD procedure, the Schwarzschild metric can be replaced in (15) for  $r > R$ , where  $p = \rho = 0$ . Since it is a solution of GR Einstein equations, it yields  $H(r > R) = 0$ . Hence the deformation  $f(r)$  in (15) is minimal,

$$f^+(r) = f(r)|_{p=\rho=H=0} = \zeta e^{-I}, \quad (19)$$

The outer radial component in Eq. (15) is given by

$$B_+(r) = 1 - \frac{2M}{r} + \zeta e^{-I}. \quad (20)$$

The parameter  $\zeta$  equals the 5D correction to the vacuum, evaluated at the star surface. Hence the MGD parameter  $\zeta$  encodes a Weyl fluid [30]. Matching conditions, for  $r < R$ , yield

$$ds^2 = A_-(r) dt^2 - \frac{dr^2}{1 - \frac{2m(r)}{r} + f^-(r)} - r^2 d\Omega^2, \quad (21)$$

where  $f^-(r)$  satisfies Eq. (15) with  $H = 0$ . Hence, for  $r > R$ , the metric, following Eq. (20), reads

$$ds^2 = A_+(r) dt^2 - \frac{dr^2}{1 - \frac{2M}{r} + f^+(r)} - r^2 d\Omega^2, \quad (22)$$

Continuity of the metric at the star surface  $r = R$ , implies

$$A_-(R) = A_+(R), \quad \frac{2M}{R} = \frac{2M_0}{R} + (f_R^+ - f_R^-), \quad (23)$$

where the sign indexes are defined by  $f_R^\pm := \lim_{r \rightarrow R^\pm} f(r)$ . Continuity of the shape tensor on  $r = R$  yields  $[G_{\mu\nu} r^\nu] = 0$ , where  $r_\mu$  is a unit radial vector, and the matching conditions at the star surface are  $[f] := \lim_{r \rightarrow R^+} f(r) - \lim_{r \rightarrow R^-} f(r)$ . Eq. (14) yields  $[\hat{T}_{\mu\nu} r^\nu] = 0$ , or equivalently,

$$\sigma p_R^- + 2 U_R^- + 4 P_R^- + \frac{(\rho_R^-)^2}{2} + p_R^- \rho_R^- = U_R^+ P_R^+, \quad (24)$$

since the star is surrounded by a Weyl fluid [22, 34].

The MGD function  $f = f^+(r)$  can be further analysed, by substituting the Schwarzschild solution in Eq. (19), yielding

$$f^+(r) = \left( 1 - \frac{2M}{r} \right) \left( 1 - \frac{3M}{2r} \right)^{-1} \frac{\zeta \ell}{r}, \quad (25)$$

where  $\ell$  is a length given by

$$\ell \equiv R \left( 1 - \frac{3M}{2R} \right) \left( 1 - \frac{2M}{R} \right)^{-1}. \quad (26)$$

<sup>1</sup> The units  $c = G = 1$  shall be adopted,  $G$  denoting the 4D Newton constant, unless otherwise specified.

In this way, the deformed outer metric reads

$$A(r) = 1 - \frac{2M}{r}, \quad (27a)$$

$$B(r) = \left(1 - \frac{2M}{r}\right) \left[1 + \zeta \left(1 - \frac{3M}{2r}\right)^{-1} \frac{\ell}{r}\right], \quad (27b)$$

enclosing the vacuum solution in Ref. [37] in the particular case when  $\zeta \ell = K/\sigma$ ,  $K > 0$ . The Weyl fluid is, hence, described by [30]

$$\begin{aligned} P^+ \sigma^{-1} &= \frac{1 - \frac{4M}{3r}}{9 \left(1 - \frac{3M}{2r}\right)^2} \frac{\zeta \ell}{r^3} \\ U^+ \sigma^{-1} &= -\frac{M}{12 \left(1 - \frac{3M}{2r}\right)^2} \frac{\zeta \ell}{r^4}. \end{aligned} \quad (28)$$

The parameter  $\zeta$  can be explicitly constructed, via the matching conditions (23) and (24), it yields  $A_-(R) = 1 - \frac{2M}{R}$ , whereas Eq. (24) yields

$$p_R + \frac{f_R^-}{R} (\ln(A(r) + r))'_{r=R} = -\frac{f_R^+}{R^2}. \quad (29)$$

The inner deformation  $f = f^-(r) > 0$ , together with the matching condition (29), shows that the outer MGD at the star surface,  $f_R^+$ , must be negative, otherwise a negative pressure  $p_R < 0$  for a solid crust would be evinced [32]. The outer geometry, governed by Eqs. (27a) and (27b), has two event horizons:

$$r_S = 2M \quad \text{and} \quad r_2 = \frac{3M}{2} - \zeta \ell. \quad (30)$$

However, one must have  $r_2 < r_S$ , since  $\zeta \sim \sigma^{-1}$  should hold in the GR limit. This implies that the outer horizon is the Schwarzschild one  $r_S = 2M$ . It is worth noting the specific value  $\zeta = -M/2$  would produce a single horizon  $r_S = 2M$ . However, the limit  $\sigma^{-1} \rightarrow 0$  does not reproduce the Schwarzschild solution, since  $M_0 = M|_{\sigma^{-1} \rightarrow 0}$ . On the other hand, the feature  $f_R^+ < 0$  implies that the deformed event horizon  $r_S = 2M$  is smaller than the Schwarzschild horizon  $r_S = 2M_0$ . Hence 5D effects weaken the strength of the gravitational field, produced by the self-gravitating compact star.

Finally, the MGD (25) and the matching condition (29) yield

$$\zeta = f_R^+ = -R^2 \left[ \left( \frac{1}{R} + \frac{A'(R)}{A(R)} \right) \frac{f_R^-}{R} + p_R \right] < 0. \quad (31)$$

In particular,  $\zeta$  can be derived by considering the exact inner brane-world solution of Ref. [22]. Now, using the explicit form of  $f = f^-(R)$  (for example, see Eq. (30) in Ref. [34]), and  $p_R = 0$  in Eq. (31), yields

$$\zeta(\sigma, R) = f_R^+ = -\frac{C_0}{R^2 \sigma}. \quad (32)$$

where  $C_0 \simeq 1.35$ . The outer geometric deformation is finally obtained by using Eq. (32) in Eq. (25), leading to

$$f^+(r) = -\frac{C_0 \ell_0}{R^2 \sigma r} \left(1 - \frac{2M_0}{r}\right) \left(1 - \frac{3M_0}{2r}\right)^{-1} + \mathcal{O}(\sigma^{-2}), \quad (33)$$

where  $\ell_0 = \ell(M_0)$ , regarding Eq. (26). In addition, 5D effects are maximal at the star surface, and more perceivable for very compact stellar distributions. Hence, the more compact the star, the larger  $|\zeta|$  is.

It is worth to mention that the brane tension  $\sigma$ , with special focus on Eqs. (32) and (33), should vary along the cosmological evolution of the Universe, since it is a scalar field [38] or an intrinsic brane feature [39, 40]. In fact, by regarding the vast variation of the temperature throughout the Universe cosmological evolution, in order to preclude global anisotropies,  $\sigma$  can be made to depend upon the cosmological time coordinate. Phenomenologically motivated Eötvös fluid membranes have tension that depend upon the temperature, as  $\sigma \sim T_0 - T$ , where  $T_0$  denotes some highest critical temperature. By disregarding bulk stresses, the bulk can be thought of as being isolated from the brane [1]. It yields the statistical mechanics equality  $dQ = dE + pdV = 0$ , where, as usual,  $Q$ ,  $E$ ,  $V$  denote, respectively, the heat, the energy and the volume content of the Universe. In addition, regarding the Cosmic Microwave Background yields [33]  $E_{\text{photons}} = \sigma T^4 V = 3p$  and, hence,  $-\frac{1}{3V} \frac{dV}{dT} = -\frac{1}{T} \frac{dT}{dt}$ . The volume is directly related to the FLRW scale factor  $a(t)$  by  $V \sim a^3(t)$ , yielding  $T \sim \frac{1}{a(t)}$  [33, 41]. Hence it implies the expression  $\sigma(t) = 1 - \frac{1}{a(t)}$ , by normalising constants, yielding  $\Lambda_{4D} \sim 1 - \frac{1}{a(t)} \left(1 - \frac{1}{a(t)}\right)$ . It means that  $\Lambda_{4D}$  had been negative, subsequently attaining positive small values, as the Universe expands, what complies to inflationary cosmology.

Some physically interesting cases are then enlisted, for the sake of illustration. For a de Sitter (dS) brane  $a(t) \sim e^{\xi t}$ ,  $\xi > 0$  [42], yielding  $\sigma(t) \sim 1 - e^{-\xi t}$ . For FLRW models, it yields  $\sigma(t) \sim 1 - t^{2/(3\gamma)}$ , where  $\gamma$  is the factor relating the density  $\rho$  to the pressure  $p$  by  $p = (\gamma - 1)\rho$ , for  $0 \leq \gamma \leq 2$  [42]. For the Milne universe, one has  $\sigma(t) \sim 1 - \alpha t$ . In particular dS branes are phenomenologically viable [1, 31], engendering a variation on the Newtonian constant  $G \sim \sigma(t)$  [33], bounded by  $\dot{G}/G \lesssim (4.0 \pm 9.1) \times 10^{-13} \text{yr}^{-1}$  was derived, from LLRE. Hence, the dS brane case yields

$$e^{\alpha t} > 1 + 10^{13} \alpha. \quad (34)$$

The standard cosmological scenario is obtained whenever  $\alpha \sim H_0$ , where  $H_0$  denotes the Hubble parameter [1], implying that  $10^{13} \alpha \sim 1$ . Moreover, there is an early time, possibly previous to the first phase transition of the Universe  $\dot{t} = \ln(1 + 10^{13} \alpha)/\alpha$ , that defines a violation of the bound (34), for any  $t < \dot{t}$ , wherein  $T \approx 1/a(t)$  [33]. Hence, the brane tension  $\sigma$  should be considered varying, along the inflation of the Universe.

## B. Casadio-Fabbri-Mazzacurati brane-world solutions

Brane Einstein field equations solutions are not solely governed by brane energy-momentum tensor. In fact, bulk gravity may impel a Weyl term on the brane. Such kind of solutions are represented by the CFM metrics [19], that are vacuum brane solutions, with PPN parameter  $\delta$ . The Nordtvedt effect provides the bound  $|\delta - 1| \lesssim 0.00023$ , whereas the observation of the deflection of light yields  $|\delta - 1| \lesssim 0.003$  [21]. The CFM metrics were derived when the constraint  $A(r) = B^{-1}(r)$  is relaxed, in Eq. (2). The CFM I solution is obtained by fixing  $A(r)$  to be equal to the analogous Schwarzschild metric coefficient and, subsequently, deriving  $B(r)$  from the Einstein field equations [20]. On the other hand, to derive the CFM II solution, the Reissner-Nordström type coefficient  $A(r)$ , representing a tidal charge, is employed [43].

For the CFM I solutions, the metric coefficients in Eq. (2) are

$$A_I(r) = 1 - \frac{2M}{r}, \quad (35)$$

$$B_I(r) = \frac{1 - \frac{3M}{2r}}{\left(1 - \frac{2M}{r}\right) \left[1 - \frac{M}{2r}(4\delta - 1)\right]} \equiv B(r). \quad (36)$$

The event horizon  $r = R$  on the brane is, hence, derived by the algebraic equation  $1/B(R) = 0$ . The sign of  $(\delta - 1)$  implies that the corresponding black hole is either colder or colder than the Schwarzschild black hole [20]. The physical singularities are governed by the singular points of curvature (Kretschmann) scalars. In fact, the coordinates  $r = 0$  and  $r = 3M/2 < R_S$  are physical singularities, wherein the scalar  $R_{\mu\nu\rho\sigma}R^{\mu\nu\rho\sigma}$  diverges. Moreover, the CFM II solution regards

$$A_{II}(r) = 1 - \frac{2M}{r} + \frac{2M^2}{r^2}(\delta - 1) \quad (37)$$

$$B_{II}(r) = B(r). \quad (38)$$

A detailed studied on the causal structure and the 5D black strings associated to both CFM solutions can be found in Refs. [3, 19, 20].

In the next section we shall apply and analyse the above described metric to study the modifications on the gravitational lensing effects, when compared to other already obtained solutions. In particular, we shall investigate the role of the PPN parameter and the brane tension in the MGD, on the observables derived in the strong field limit.

## IV. OBSERVABLES IN THE STRONG FIELD LIMIT

One of the important aspects of the SFL approach is the potential to identify different black hole solutions. However, the applicability of the approach is hugely increased by the possibility of testing extensions of GR. In

fact, any testable features of theories beyond GR could provide us important hints on the nature of gravity, in such regimes. Our aim, in this section, is to identify the deviation of the MGD and CFM solutions from the classical Schwarzschild black hole. It is accomplished by analysing the observables of the SFL found in Ref. [13] and, subsequently, comparing them with the standard Schwarzschild one.

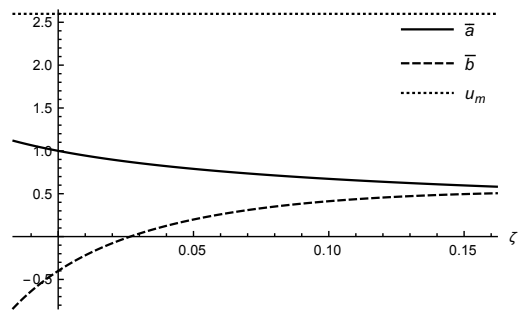


FIG. 2: SFL coefficients for the MGD solution as a function of the parameter  $\zeta$  in Eq. (32).

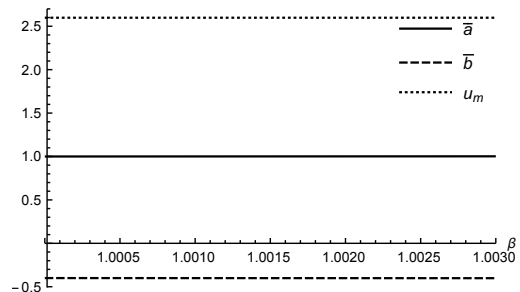


FIG. 3: SFL coefficients for the CFM I solution, as a function of the PPN parameter  $\delta$ .

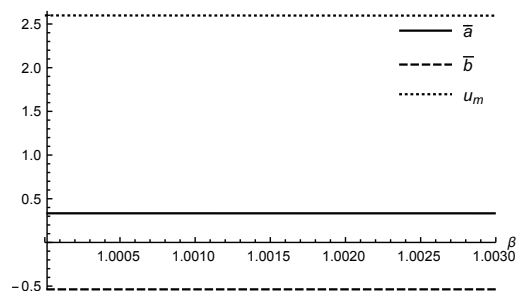


FIG. 4: SFL coefficients for the CFM II solution, as a function of the PPN parameter  $\delta$ .

It is worth to mention that the lines in Figs. 3 and 4 are not really straight, but just a resolutional consequence of the tiny range determined by the (currently observed) PPN parameter  $\delta$ , in Figs. 2 – 4. Some ob-

servable features of the SFL regime can be calculated, by using only the expansion coefficients, namely,  $\bar{a}$ ,  $\bar{b}$ , respectively in Eqs. (5) and (6), and  $u_m = r_m/A(r_m)$  [13]. Fig. 2 shows their behaviour, upon varying the parameter  $\zeta$  of the MGD solution. Figs. 3 and 4 show that the coefficients do not have an appreciable variation, in the allowed range of the parameter  $\delta$ , for the CFM I and CFM II solutions, as showed in Table II.

The first observable is related to the distance of relativistic images, being defined as the angular distance  $s$  between the largest and smallest orbit of the light rays winding around the black hole. The second is the angular position  $\theta_\infty$  of the accumulating relativistic images. The third one is the magnification of the images after of the lensing effect. The details of the derivation of those observables are not very involved, however here we are going to sketch those derivations, referring to the original paper for more details.

Despite of the angle  $\theta$  between the lens, and the image being large in the SFL, the effects are more prominent when the source, the lens, and the observer are highly aligned [11]. It means that the deflection angle  $\alpha$  should be a small deviation of  $2n\pi$ , that is  $\alpha(\theta) = 2n\pi + \Delta\alpha_n$ , with  $\Delta\alpha_n$  small. The next step is to find the angles  $\theta_n^0$  such that  $\alpha(\theta_n^0) = 2n\pi$ , which represents a deviation  $\Delta\alpha_n$ , and expand  $\alpha(\theta)$  around  $\theta_n^0$ . Hence, the lens equation (4) straightforwardly yields

$$\theta_n^0 = \frac{u_m}{D_{ol}} \left[ 1 + \exp\left(\frac{\bar{b} - 2n\pi}{\bar{a}}\right) \right] \quad (39)$$

resulting in

$$\Delta\alpha_n = \frac{\bar{a}D_{ol}}{u_m \exp\left(\frac{\bar{b} - 2n\pi}{\bar{a}}\right)} (\theta_n^0 - \theta). \quad (40)$$

It allows us to define the two following observables,

$$\theta_\infty \equiv \lim_{n \rightarrow \infty} \theta_n^0 = \frac{u_m}{D_{ol}}, \quad (41)$$

$$s \equiv \theta_1 - \theta_\infty = \theta_\infty \exp\left(\frac{\bar{b} - 2\pi}{\bar{a}}\right). \quad (42)$$

The magnification resulting from the lensing effect, defined as the ratio of the flux of the image to the flux of the unlensed source [11], is the third observable quantity in the SFL regime. Given the flux

$$\mu = \frac{\sin \theta}{\sin \beta} \left( \frac{d\beta}{d\theta} \right)^{-1}, \quad (43)$$

the ratio of flux of the images to the flux of the source, expressed as function of the SFL coefficients, reads [13, 18]

$$k = \frac{\mu_1}{\sum_{n=2}^{\infty} \mu_n} = \exp\left(\frac{2\pi}{\bar{a}}\right). \quad (44)$$

Now we can use the known data from the galactic supermassive black hole at the centre of our galaxy, to compare SFL lensing results of the Schwarzschild, MGD and CFM solution. The observables and the SFL coefficients for MGD and CFM solutions are displayed in the Tables I & II. In both cases we calculated the results considering the allowed range of the parameter  $\zeta$  for the MGD metric and the  $\delta$  for the CFM metrics. The mass of this supermassive black hole and its distance from the Earth used in the calculations are  $M = 2.8 \times 10^6 M_\odot$  and  $D_{ol} = 8.5\text{kpc}$  respectively. In what follows, the value  $R = 1.437R_S$  regarding the MGD solutions shall be taken into account in  $\zeta$ , corresponding to a compact object surface, by considering the current value for the cosmological constant in the matching conditions at the surface. In addition, in the tables below we denote, as usual, by  $s = \theta_1 - \theta_\infty$  the angular difference from the outmost image and the adherent point formed by the others for  $n \rightarrow \infty$ ;  $k_m = 2.5 \log k$  denotes the magnitude;  $u_m/R_S$  is the normalised minimum impact parameter;  $\bar{a}$  and  $\bar{b}$  denote strong field limit coefficients that constitute the deflection angle.

	Schwarzschild	MGD					
	( $\zeta \equiv 0$ )	$\zeta = -1.69 \times 10^{-2}$	$1.31 \times 10^{-2}$	$4.31 \times 10^{-2}$	$7.31 \times 10^{-2}$	$10.31 \times 10^{-2}$	$13.31 \times 10^{-2}$
$\theta_\infty$ ( $\mu\text{arcsec}$ )	16.87	16.87	16.87	16.87	16.87	16.87	16.87
$s$ ( $\mu\text{arcsec}$ )	0.0021	0.0291	0.0162	0.0088	0.0047	0.0026	0.0014
$k_m$	6.82	6.09	7.34	8.41	9.36	10.22	11
$u_m/R_S$	2.6	2.6	2.6	2.6	2.6	2.6	2.6
$\bar{a}$	1	1.12	0.93	0.81	0.73	0.67	0.62
$\bar{b}$	-0.4002	-0.8459	-0.1715	0.1499	0.3225	0.4203	0.4759

Table I. Observables in the strong field limit for the MGD solution.

	Schwarzschild ( $\delta \equiv 1$ )	CFM I			CFM II		
		$\delta = 1.001$	1.002	1.003	$\delta = 1.001$	1.002	1.003
$\theta_\infty$	16.87	16.87	16.87	16.87	16.87	16.86	16.85
$s$	0.0211	0.0212	0.0213	0.0214	$\sim 10^{-8}$	$\sim 10^{-8}$	$\sim 10^{-8}$
$k_m$	6.82	6.817	6.813	6.808	20.473	20.479	20.486
$u_m/R_S$	2.6	2.6	2.6	2.6	2.6	2.6	2.6
$\bar{a}$	1	1.0007	1.0013	1.0020	0.3332	0.3331	0.333
$\bar{b}$	-0.4002	-0.4007	-0.4011	-0.4016	-0.5371	-0.537	-0.537

Table II. Observables in the strong field limit for both the CFM solutions.

## V. CONCLUDING REMARKS AND OUTLOOK

The effects of gravitational lensing in the strong field regime are concretely noticeable, at least theoretically, wherein the thorough capture of the photon by the black hole is regarded. The so-called inversion problem is capable to uniquely determine the nature of the black hole, from the parameters associated with the successive images formation, as their relative distances, the asymptotic position approached by the set of images, and their measured positions, accordingly. Regarding both the CFM solutions, and the MGD of GR, we calculated the observables of the gravitation lensing of a background source in the strong field regime. The angular difference  $s$  from the outmost image and the adherent point formed by the other images; the parameter  $k_m$  that reveals the image magnification; the normalised minimum impact parameter  $u_m/R_S$  were studied, unraveling a precise observable signature for the CFM I, the CFM II, and the MGD solutions, that may model the supermassive black hole in the centre of our galaxy. Based upon the satellite mission of the ESA of astrometric measurements, the accuracy can reach  $7 \mu\text{as}$  [44], the typical signature of CFM

I, CFM II, and MGD solutions are, mainly, observable by the parameters  $k_m$  and  $\theta_\infty$ . It is worth to mention that the CFM II solution is hugely different, when compared to the Schwarzschild, CFM I, and MGD solutions, in what regards the parameter the magnitude  $k_m$ . This analysis was presented and encrypted in Tables I – for different values of the brane tension, according to Eq. (32), and II (for different values of the PPN parameter. The signatures of the MGD, on the other hand, could be evinced by the combinations of the parameters  $k_m$  and  $s$ . However, even the difference on the values of  $s$  for the MGD and Schwarzschild being higher than one order of magnitude, it is still a little beyond the current ESA resolution. Thus, from the observational perspective, astrophysical data should be better improved, in order to apply the thorough potential of the gravitational lensing, in the strong field regime.

### Acknowledgements

RTC and AGS are supported by CAPES. RdR is grateful to CNPq (grants No. 303293/2015-2 and No. 473326/2013-2), and to FAPESP (grant No. 2015/10270-0), for partial financial support.

- 
- [1] Maartens R and Koyama K 2010 *Living Rev. Rel.* **13** 5 (*Preprint* 1004.3962)
  - [2] Dimopoulos S and Landsberg G L 2001 *Phys. Rev. Lett.* **87** 161602 (*Preprint* hep-ph/0106295)
  - [3] da Rocha R, Piloyan A, Kuerten A M and Coimbra-Araujo C H 2013 *Class. Quant. Grav.* **30** 045014 (*Preprint* 1301.4483)
  - [4] Dyson F W, Eddington A S and Davidson C 1920 *Phil. Trans. Roy. Soc. Lond.* **A220** 291
  - [5] Zwicky F 1937 *Phys. Rev.* **51** 290
  - [6] Liebes S 1964 *Phys. Rev.* **133** B835
  - [7] Refsdal S 1964 *Mon. Not. Roy. Astron. Soc.* **128** 295
  - [8] Walsh D, Carswell R F and Weymann R J 1979 *Nature* **279** 381
  - [9] Paczynski B 1987 *Nature* **325** 572–573
  - [10] de Xivry G O and Marshall P 2009 *Mon. Not. Roy. Astron. Soc.* **399** 2 (*Preprint* 0904.1454)
  - [11] Virbhadra K S and Ellis G F R 2000 *Phys. Rev.* **D62** 084003 (*Preprint* astro-ph/9904193)
  - [12] Bozza V, Capozziello S, Iovane G and Scarpetta G 2001 *Gen. Rel. Grav.* **33** 1535 (*Preprint* gr-qc/0102068)
  - [13] Bozza V 2002 *Phys. Rev.* **D66** 103001 (*Preprint* gr-qc/0208075)
  - [14] Keeton C R and Petters A O 2005 *Phys. Rev.* **D72** 104006 (*Preprint* gr-qc/0511019)
  - [15] Keeton C R and Petters A O 2006 *Phys. Rev.* **D73** 044024 (*Preprint* gr-qc/0601053)
  - [16] Keeton C R and Petters A O 2006 *Phys. Rev.* **D73** 104032 (*Preprint* gr-qc/0603061)
  - [17] Whisker R 2006 Gravitational lensing by braneworld black holes *Recent developments in theoretical and experimental general relativity, gravitation and relativistic field theories. Proceedings, 11th Marcel Grossmann Meeting, MG11, Berlin, Germany, July 23-29, 2006. Pt. A-C* p 1707
  - [18] Bozza V 2010 *Gen. Rel. Grav.* **42** 2269 (*Preprint*

- 0911.2187)
- [19] Casadio R and Mazzacurati L 2003 *Mod. Phys. Lett.* **A18** 651 (*Preprint* gr-qc/0205129)
- [20] Casadio R, Fabbri A and Mazzacurati L 2002 *Phys. Rev.* **D65** 084040 (*Preprint* gr-qc/0111072)
- [21] Will C M 2006 *Living Rev. Rel.* **9** 3 (*Preprint* gr-qc/0510072)
- [22] Ovalle J 2009 *Int. J. Mod. Phys.* **D18** 837 (*Preprint* 0809.3547)
- [23] Casadio R, Ovalle J and da Rocha R 2015 *Class. Quant. Grav.* **32** 215020 (*Preprint* 1503.02873)
- [24] Ovalle J 2008 *Mod. Phys. Lett.* **A23** 3247 (*Preprint* gr-qc/0703095)
- [25] Carroll S M 2004 *Spacetime and geometry: An introduction to general relativity* (Addison-Wesley, San Francisco, 2004)
- [26] Weinberg S 1972 *Gravitation and cosmology: principles and applications of the general theory of relativity* vol 1 (Wiley New York)
- [27] Whisker R 2005 *Phys. Rev.* **D71** 064004 (*Preprint* astro-ph/0411786)
- [28] Majumdar A S and Mukherjee N 2005 *Mod. Phys. Lett.* **A20** 2487 (*Preprint* astro-ph/0403405)
- [29] Boehmer C G, De Risi G, Harko T and Lobo F S N 2010 *Class. Quant. Grav.* **27** 185013 (*Preprint* 0910.3800)
- [30] Casadio R, Ovalle J and da Rocha R 2015 *Europhys. Lett.* **110** 40003 (*Preprint* 1503.02316)
- [31] Shiromizu T, Maeda K i and Sasaki M 2000 *Phys. Rev.* **D62** 024012 (*Preprint* gr-qc/9910076)
- [32] Ovalle J, Gergely L and Casadio R 2015 *Class. Quant. Grav.* **32** 045015 (*Preprint* 1405.0252)
- [33] da Rocha R and Hoff da Silva J M 2012 *Phys. Rev.* **D85** 046009 (*Preprint* 1202.1256)
- [34] Casadio R, Ovalle J and da Rocha R 2014 *Class. Quant. Grav.* **31** 045016 (*Preprint* 1310.5853)
- [35] dos Anjos R C, Coimbra-Araujo C H, da Rocha R and de Souza V 2016 *JCAP* **1603** 014 (*Preprint* 1510.04992)
- [36] Casadio R and Ovalle J 2014 *Gen. Rel. Grav.* **46** 1669 (*Preprint* 1212.0409)
- [37] Germani C and Maartens R 2001 *Phys. Rev.* **D64** 124010 (*Preprint* hep-th/0107011)
- [38] Bergshoeff E and Townsend P K 1998 *Nucl. Phys.* **B531** 226 (*Preprint* hep-th/9804011)
- [39] Gergely L A 2008 *Phys. Rev.* **D78** 084006 (*Preprint* 0806.3857)
- [40] Hoff da Silva J M 2011 *Phys. Rev.* **D83** 066001 (*Preprint* 1101.4214)
- [41] Gergely L A 2009 *Phys. Rev.* **D79** 086007 (*Preprint* 0806.4006)
- [42] Campos A and Sopena C F 2001 *Phys. Rev.* **D63** 104012 (*Preprint* hep-th/0101060)
- [43] Dadhich N, Maartens R, Papadopoulos P and Rezanian V 2000 *Phys. Lett.* **B487** 1 (*Preprint* hep-th/0003061)
- [44] Jordan S 2008 *Astron. Nachr.* **329** 875 (*Preprint* 0811.2345)